World Applied Sciences Journal 14 (9): 1406-1414, 2011
ISSN 1818-4952

Implementation of a Full Bridge Series-Parallel Resonant DC-DC Converter Using Artificial Neural Networks and Sequential State Machine Controllers

[1]*Mohammad Jafari,* [2]*Zahra Malekjamshidi and* [1]*Mohsen Imanieh*

[1]Department of Electrical and Electronic Engineering, Fasa branch,
Islamic Azad University, Fasa, Iran
[2]Department of Electrical and Electronic Engineering, Marvdasht Branch,
Islamic Azad University, Marvdasht, Iran

Abstract: In this paper, two methods of control for high-voltage Full Bridge Series-Parallel Resonant (FBSPR) DC-DC converter are proposed and the results are compared. Soft switching operation using Zero Current Switching (ZCS) and Zero Voltage Switching (ZVS) technologies is employed to decrease the losses and optimize the efficiency of converter. The way of obtaining small-signal model of FBSPR converter using the generalized averaging method is discussed. Then two control methods using Artificial Neural Networks (ANN) and Sequential State Machine (SSM) are explained and the experimental results are compared. The ANN controller is trained according to the small signal model of the converter and operating points and the SSM controller operates on base of a finite number of states, actions and functions and determines transition from one state to another according to FBSPR converter conduction status. To compare the performances of two controllers, a prototype is designed and implemented. The prototype is tested for step changes in both output load and reference voltage at steady state and under transient conditions. Comparison between experimental results for both ANN and SSM controllers show better speed performances for SSM controller in small changes in load and more reliability for ANN controller in case of large variations.

Key words: Full Bridge · Series-Parallel Resonant Converter · Artificial Neural Networks · Sequential State Machine · ZVS · ZCS

INTRUDUCTION

The design and analysis of resonant converters is often complex due to the large number of operating states occurring within a pulse period. In this paper a Full Bridge Series-Parallel Resonant (FBSPR) Converter using two control methods are introduced. They are based on Neural Networks and Sequential State Machine. The different steps of design, simulation and experimental tests are discussed. The converter output power is controlled by duty-cycle variation while the switching frequency should be adjusted to ensure that one bridge leg commutates at zero current (ZCS). The second bridge leg operates under zero voltage switching condition (ZVS) and this guarantees the soft-switching operation in the entire operating range [2].To design an appropriate controller, an accurate small signal model of the converter is needed. Many controllers are designed by trial and error methods and this takes some time to set the controller parameters [3].

In this paper a generalized averaging method is used to obtain the small signal model [4, 2]. This method overcomes the limitations of the traditional state-space averaging method because it does not require that the waveforms have small ripple magnitude. Thus, it is able to describe arbitrary types of waveforms [2]. As this model doesn't need complex mathematical analysis, it simplifies the controller design for FBSPR converters and minimizes the design time, especially in the trial and error methods. Different adaptive controllers for the FBSPR Converter is suggested, such as Gain Scheduled controller [6, 2], Passivity Based controller[7][8], Sequential State Machine [2, 5] and Fuzzy Controller. The Gain scheduling is a feed forward adaptation and it can be regarded as a mapping from process to controller parameters. The main advantage of gain scheduling is the fast dynamic response of the controller. The Passivity based control is a very robust method but its dynamic response is not as fast as the response of the gain scheduled controller

Corresponding Author: Mohammad Jafari, Department of Electrical and Electronic Engineering,
Islamic Azad University- Fasa branch, Fasa, Fars province, Iran. Tel/Fax : +989173036085.

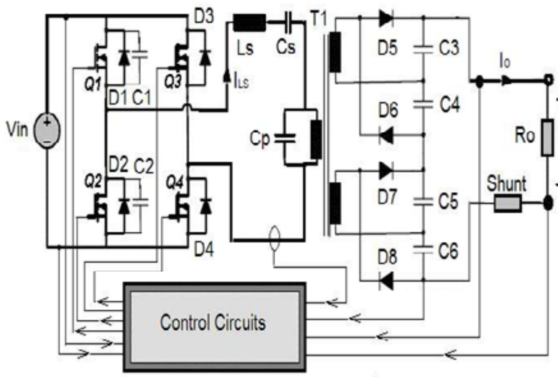

Fig. 1: Structure of purposed FBSPR converter

because it depends on the speed of the estimate of the load [2,7]. The Sequential State Machine is an abstract machine composed of finite number of states that determines transition from one state to another [2]. It provides the gate signals for power switches according to the previous value of some power circuit parameters [2] [5]. In this paper two ANN and SSM based controllers are employed to provide a safe and stable response during any variation in output voltage in case of any changes in load or reference voltage. A prototype also is implemented to obtain experimental results on base of a high speed Digital Signal Processor (DSP). Figure 1 shows the structure of the FBSPR Converter. The block known as Control Circuits provides the gate driving signals according to several electrical signals from power circuits.

In the Following sections, the steady state analysis of FBSPR Converter is reviewed in section B, the small signal model is discussed in section C. section D allocated to the ANN and SSM controllers and simulation and experimental results are discussed in sections E and F.

Steady State Analysis of FBSPR Converter: The FBSPR Converters can operate in three commutation mode known as Natural, Forced and Mixed modes [2]. In the natural mode transistors operate with Zero Current Switching (ZCS) in the turn off time. To reduce the turn off losses, fast recovery diodes should be used as the current spikes take place during the turn off process [2, 9]. In the forced mode all switches operate with Zero Voltage Switching (ZVS) and turn on when their anti-parallel diodes are in conduction mode and turn off with current [2]. In the mixed mode, switches of one bridge legs (Q1,Q2) work with the ZVS during turning on and the switches of other legs (Q3,Q4) operate in ZCS during turning off time. In this mode the conduction losses are minimized and the converter efficiency increases. In our project the converter works in boundary between forced and mixed commutation modes. In this mode the switches Q3 and Q4 turn on and off with zero current and the switches Q1 and Q2 turn on with ZVS according to operation above resonant frequency [2]. The resonant current I_{LS} is almost sinusoidal form during the operation and so its spectrum contains only the first harmonic component. However waveforms of V_{AB} and I'_D do not have sinusoidal form.

The voltage transfer ratio of the resonant converter $G(s)$ can be calculated as a function of the output rectifier conduction angle (which is proportion to load variations) and the normalized switching frequency according to equation (1) [2].

$$G(s) = {v_o}/{v_{in}} = n\frac{4}{\pi}.\frac{K}{K'} \tag{1}$$

In this equation n is high frequency transformer ratio, K and K' are defined as:

$$K = \left[\left[1 - \frac{C_p}{C_s}\left((\frac{f_s}{f_o})^2 - 1 \right)\right]. \left(1 + \frac{\tan \; ({C_P}/{C_S})}{\omega.C_p.R_e} \right)]^2 + \left[\frac{C_p}{C_s}.\left((\frac{f_s}{f_o})^2 - 1 \right) \right] \right]^{-1/2} \tag{2}$$

$$K' = 1 + 0.27 Sin\left({\varphi}/{2} \right) \tag{3}$$

Where, φ is the conduction angle of output rectifier which changes according to load variations, f_s denotes the switching frequency and f_o is the series resonant frequency and is calculated according to equation (4).

$$f_0 = 2\pi \left(L_S C_S \right)^{-1/2} \tag{4}$$

Figure 2 presents the three dimensional graph of $G(s)$ as a function of $\left({f_S}/{f_o} \right)$ and load variations (φ).

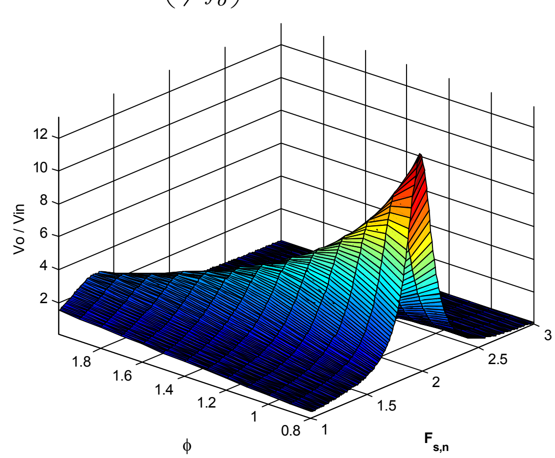

Fig. 2: Three dimensional graph of G(s) as a function of ${f_S}/{f_o}$ and load variation (φ)

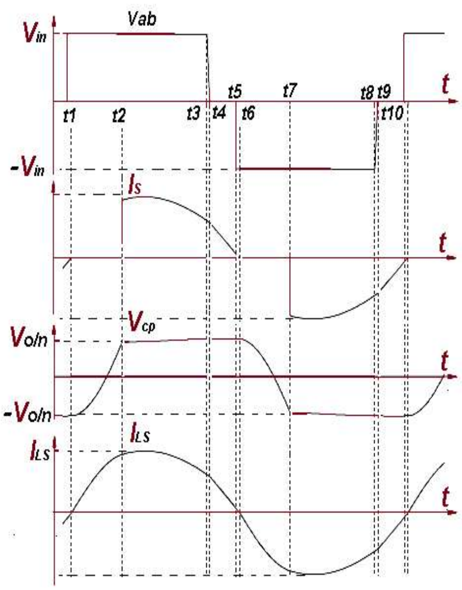

Fig. 3: Waveforms of converter during a period

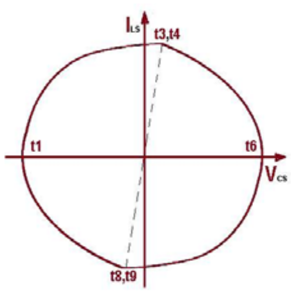

Fig. 4: The steady state trajectory for state variables of converter

The resonant frequency of the circuit (f_o) changes with the conduction angle (φ) and load variations. This is because of the influence C_p on the resonant frequency. The converter behaves as a series resonant converter at lower frequencies and as a parallel resonant converter at higher frequencies [2]. When the resonant current flows for only a small part of the switching period through C_p and the load is increased, the converter behaves as a series resonant converter. In this case the resonant frequency is almost equal to the series resonant frequency (f_o). On the other hand, the converter behaves as a parallel resonant converter in low loads and while current flows almost the whole switching period through Cp [2, 10].

In the following sections, the operation of the series-parallel resonant converter above resonance with variable frequency and phase-shift control is explained in details. In this paper, FBSPR converter switches commutate in a boundary between mixed and forced modes to combine the advantage of both commutation modes.

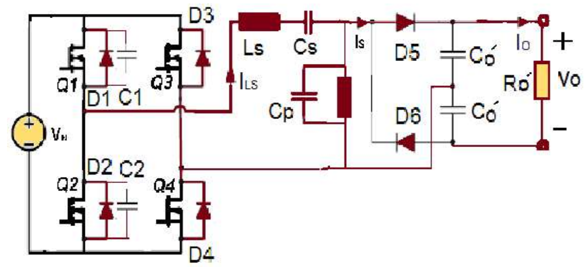

Fig. 5: The equivalent circuit of FBSPR converter for small signal analysis

This mode of operation was described in [2]. Figure 3 illustrates the waveforms of converter during a pulse period from t1 to t10 and it is obvious that resonant current is almost in sinusoidal form. The steady state trajectory for the FBSPR converter operating at full load is shown in figure 4. It is obvious that the shape of the trajectory is almost circular which means that the state variables of the converter circuit (ILS, VCS) are almost in sinusoidal form. The times shown in the diagram are referred to figure 3. In the next section, the steady state small signal model for FBSPR converter is obtained and analyzed.

Small Signal Model: In order to find the small-signal model for the FBSPR converter with capacitive output filter, the first step is to find an equivalent circuit. In this circuit the components in secondary side of high frequency transformer referred to the primary side as shown in figure 5. The state variables of the circuit considering the fundamental harmonics of ILS and VCS are defined as [1,2].

$$\langle I_{LS} \rangle_1 = x_1 + jx_2 \tag{5}$$

$$\langle V_{CS} \rangle_1 = x_3 + jx_4 \tag{6}$$

$$\langle V_{CP} \rangle_1 = x_5 + jx_6 \tag{7}$$

$$\langle V_{O'} \rangle_0 = x_7 \tag{8}$$

Where x_1, x_3 and x_5 are representative of cosine components of waveforms and x_2, x_4 and x_6 for sinusoidal parts. The state variables x_5 and x_6 are written as a function of x_1 and x_2 as they are representative of parallel capacitor voltage which could not be considered as a state variable.

$$x_5 = \frac{1}{\pi \omega_s C_P}\left[x_1 \delta + x_2 \gamma\right] \tag{9}$$

$$x_6 = \frac{1}{\pi\omega_s C_P}\left[x_2\delta - x_1\gamma\right] \quad (10)$$

Where

$$\gamma = \pi - \varphi + \frac{1}{2}Sin(2\varphi) \quad (11)$$

$$\delta = Sin^2(\varphi) \quad (12)$$

According to these variables, the state vector of circuit can be written as:

$$x = [x_1 \quad x_2 \quad x_3 \quad x_4 \quad x_5]^T \quad (13)$$

Where:

$$\frac{dx_1}{dt} = \omega_s x_2 - \frac{x_3}{L_s} - \frac{x_5}{L_s} + \frac{V_{in}Sin(D\pi)}{\pi L_s} \quad (14)$$

$$\frac{dx_2}{dt} = -\omega_s x_1 - \frac{x_4}{L_s} - \frac{x_6}{L_s} + \frac{V_{in}}{\pi L_s}\left(Con\left(D\pi\right)-1\right) \quad (15)$$

$$\frac{dx_3}{dt} = \omega_s x_4 + \frac{x_1}{C_s} \quad (16)$$

$$\frac{dx_4}{dt} = -\omega_s x_3 + \frac{x_2}{C_s} \quad (17)$$

$$\frac{dx_7}{dt} = \frac{2\sqrt{x_1^2+x_2^2}}{\pi C_{o'}}.\left[1-Cos\left(\varphi\right)\right] - \frac{2x_7}{R_{o'}.C_{o'}} \quad (18)$$

In these equations ω_s (switching frequency) is selected as u_1 (first control input variable) and D (duty cycle of switching pulses) as u_2 (second control input). On the other side the output voltage, the amplitudes of ILS and VCS are selected as output variables y_1, y_3 and y_3 respectively. Therefore the relation between state variables, control inputs and outputs can be written as follow:

$$u_1 = \omega_s \quad (19)$$

$$u_2 = D \quad (20)$$

$$y_1 = x_7 \quad (21)$$

$$y_2 = 2\sqrt{x_1^2 + x_2^2} \quad (22)$$

$$y_3 = 2\sqrt{x_3^2 + x_4^2} \quad (23)$$

To obtain a steady state solution of the system and finding the small signal model, the derivatives of Equations (14)-(18) should be equal to zero. Furthermore, the equations providing the steady state solution can be achieved using (φ_{ss}), the steady state value of φ according to below equations.

$$\varphi_{ss} = 2.\tan^{-1}\sqrt{\frac{2\pi}{\omega_s C_p R_{o'}}} \quad (24)$$

$$\gamma_{ss} = \pi - \varphi_{ss} + \frac{1}{2}Sin(2\varphi_{ss}) \quad (25)$$

$$\delta_{ss} = Sin^2\left(\varphi_{ss}\right) \quad (26)$$

$$K = \frac{\omega_{S_{ss}}.C_p.V_{in}}{\delta_{ss}} \quad (27)$$

$$M = \frac{\delta_{ss}}{\gamma_{ss} + \pi(C_p/C_s) - \pi\omega_{ss}^2.L_s.C_p} \quad (28)$$

$$x_{1_{ss}} = -\frac{x_{2_{ss}}}{M} + K.Sin(D\pi) \quad (29)$$

$$x_{2_{ss}} = \frac{K.M^2}{(1+M^2)}\left[\frac{Sin(D.\pi)}{M} + \{Cos(D\pi)-1\}\right] \quad (30)$$

$$x_{3_{ss}} = \frac{x_{2_{ss}}}{\omega_{s_{ss}}.C_s} \quad (31)$$

$$x_{4_{ss}} = -\frac{x_{1_{ss}}}{\omega_{s_{ss}}.C_s} \quad (32)$$

$$x_{5_{ss}} = \frac{1}{\pi.\omega_{s_{ss}}.C_p}\left[x_{1_{ss}}.\delta_{ss} + x_{2_{ss}}.\gamma_{ss}\right] \quad (33)$$

$$x_{6_{ss}} = \frac{1}{\pi.\omega_{s_{ss}}.C_p}\left[x_{2_{ss}}.\delta_{ss} - x_{1_{ss}}.\gamma_{ss}\right] \quad (34)$$

$$x_{7_{ss}} = \frac{R_{o'}\sqrt{x_{1_{ss}}^2 + x_{2_{ss}}^2}}{\pi}\left[1-Cos(\varphi_{ss})\right] \quad (35)$$

The small signal transfer function was achieved after linearization of model around the steady state. The linearized model according to below equations can give $G(S)$ which is ratio of output voltage to duty cycle.

$$\Delta\dot{\vec{x}} = A.\Delta\vec{x} + B.\Delta\vec{u} \quad (36)$$

$$\Delta\vec{y} = C.\Delta\vec{x} + D.\Delta\vec{u} \quad (37)$$

Where A, B, C and D are matrices of system parameters and $\vec{x}$, $\vec{y}$ and $\vec{u}$ are state, output and input vectors respectively. The symbol Δ means small changes in respective parameter.

$$G(S) = \frac{\Delta V_O}{\Delta D} = \frac{\Delta y_1}{\Delta u_2} \quad (38)$$

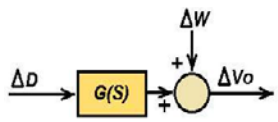

Fig. 6: Block diagram of system model

Table 1: State transition table for conduction

Switchcurrent State	ZVS-HI	ZVS_LO	ZCS_HI	ZCS_LO
ST1	OFF	ON	ON	OFF
ST2	ON	OFF	ON	OFF
ST3	ON	OFF	OFF	ON
ST4	OFF	ON	OFF	ON
ST5	OFF	OFF	OFF	OFF
ST6	OFF	OFF	OFF	ON
ST7	OFF	OFF	ON	OFF
Error	OFF	OFF	OFF	OFF

To achieve a complete model of system, variation of switching frequency can be modeled by a constant disturbance because of its instantaneous changes. It automatically adjusted to ensure ZCS operation of one bridge leg. The finalized model is shown in figure 6. It can be used as an ideal model to produce sample data for training ANN controller in the next stage.

Design of Ann and Ssm Controllers: In this section the design procedures for both Artificial Neural Network (ANN) and Sequential State Machine (SSM) base controllers will be described in brief.

Design of SSM Controller: Several conduction modes took place during a complete switching period. Each state distinguishes by the transistors and diodes which conduct during their respected time. In general there are normally four basic states but several unexpected or unwanted states may also take place which should be considered and included into the state table. The SSM controller is an abstract machine which determines transition from one operating states of converter to another on base of satisfaction of several conditions. The operation states are illustrated in a state transition table 1.

The controller would determine what state the converter switches should move to. This guarantees a proper operation for power circuit of converter. To implement this control strategy, a Sequential State Machine (SSM) controller is designed to operate according to below state diagram. The state diagram is adapted to state transition table.

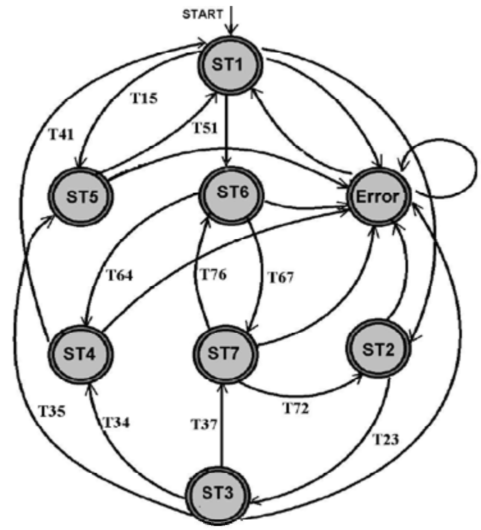

Fig. 7: State diagram of sequential state machine

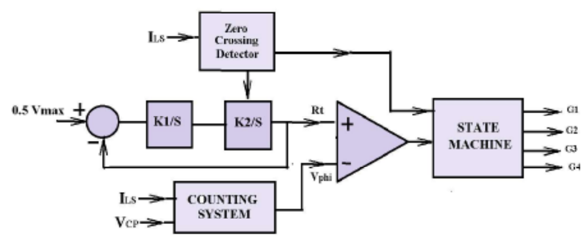

Fig. 8: The constant amplitude sawtooth signal generator

The diagram in practice is realized through several simple software loops. The SSM has eight states (ST1,ST2,ST3,ST4,ST5,ST6,ST7,Error) which switches are turned on or off for each state conduction [2]. The control process starts at state ST1 which two diagonal switches are on. This applies the full input voltage across the resonant circuit, transferring power to the load. The normal operation states are ST1, ST2, ST3 and ST4. ST5 is related to discontinuous mode state and ST6 and ST7 are special states to prevent operation below resonance. There is a transition from each state to the Error state, if some abnormal behavior occurs [2]. In this case, all switches are turned off and the state machine can be restart from state (st1).

In this controller, the switches Q3 and Q4 turn on and off with zero crossing of current (ILS) and the switches Q1 and Q2 turn on with ZVS according to operation above resonant frequency and synchronize with zero crossing of ILS. The gate drive signals of Q1 and Q2 are generated by comparing a constant amplitude sawtooth-shaped signal (Rt) and a computed variable voltage (Vphi). The sawtooth signal with constant amplitude is generated according to below circuit [2].

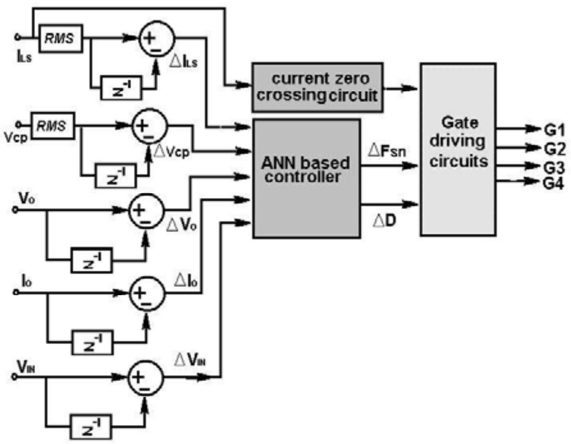

Fig. 9: The overall structure of ANN controller

The frequency of sawtooth-shaped signal changes according to output voltage and current variations to guarantee the operation above resonant frequency. The amplitude of voltage (Vphi) is computed according to changes in state variables of resonant circuit (ILS, VCP). The resulted PWM voltage transferred to SSM controller to provide the gate drive signals of switches.

Design of ANN Controller: The second controller is an Artificial Neural Network which is trained according to an ideal simulated model of FBSPR converter. In this research, a multi-layer feed-forward artificial neural network is employed to achieve real-time control. Since the output voltage is a nonlinear function of duty cycle (ΔD) and switching frequency ($\Delta Fs,n$), they are chosen to be the outputs of the neural network controller. The input variables of ANN are, input voltage (Vin), output current (I0), output DC voltage (Vo), series inductor current (I_{LS}) and parallel capacitor voltage (Vcp) as storage elements. The converter output voltage should be kept at a constant while the ZVS and ZCS operation should be guaranteed; otherwise, the duty cycle of control signal should be changed for both line and load regulations and the switching frequency should be changed for ZVS operation. Therefore, the outputs of the ANN controller are the changes in duty cycle and frequency of driving signals ($\Delta D, \Delta Fs,n$). The overall structure of designed controller illustrated in figure 9. The ANN based controller is trained according to an ideal simulated model of FBSPR converter. The ideal model is simulated using small signal equations of the system as described in section (C). At the first step, a simulated model using MATLAB software is developed to represent the converter system and it is used to evaluate the converters states and outputs at any time. Then we apply changes to the input controller parameters and search by an offline iteration procedure, at each sampling point. This process gives us the exact values of the control variables needed to ensure convergence of output signals to the desired values at the next sampling point. The obtained ideal control signals which are the desired ANN inputs and outputs are saved as a training data set. The data set is then used to train the ANN to mimic the behavior of the ideal controller. In order to satisfy this requirements, a multi-layer feed-forward ANN, was selected to be trained. It is clear that a multi-layer feed-forward ANN can approximate any nonlinear function. The nonlinear sigmoid function is chosen as the activation function [9].

$$f(x) = 1 \big/ 1 + e^{-ax} \quad (39)$$

After simulation of converter according to small signal model and training of ANN controller, sensitivity based neural network pruning approach is employed to determine an optimal neural network controller configuration [9]. In this approach, the contribution of each individual weight to the overall neural network performance is indicated by a sensitivity factor $j(w_{ij})$. The sensitivity of a global error function, with respect to each weight, S_{ij} can be defined as the following [9]:

$$\begin{aligned} S_{ij} &= J(w_{ij}=0) - J(w_{ij}=w_{ij}^{f}) \\ S_{ij} &= J(without\ w_{ij}) - J(with\ w_{ij}) \end{aligned} \quad (40)$$

In these equations, w_{ij} is the weight of the neural network and w_{ij}^{f} is the final value of weight after training. The equation (40) can be approximated by (41) for the back-propagation algorithm [9].

$$S_{ij} \approx \sum_{n=1}^{N} \left[\Delta w_{ij}(n)\right]^2 \frac{w_{ij}^{f}}{\eta(w_{ij}^{f} - w_{ij}^{i})} \quad (41)$$

Where N is the number of training patterns for each ANN weight update, η is the learning rate which is chosen to be 0.6 and ΔW_{ij} is the weight update. The sensitivity calculations were done on based of Equation (41). The weights are insignificant and can be deleted if their sensitivity factor was smaller than a defined threshold and also a neuron can be removed when the sensitivities of all the weights related with this neuron are below than the threshold [9]. This process reduced the number of active weights and neurons and was effective in development of

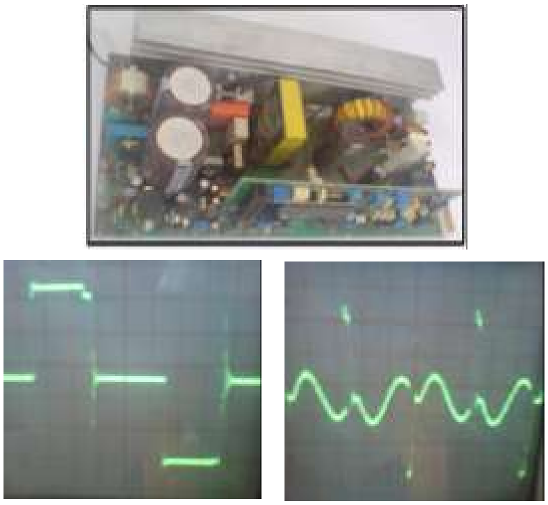

Fig. 10: a) The implemented FBSRP converter
b) Wave forms of VAB for full and light loads

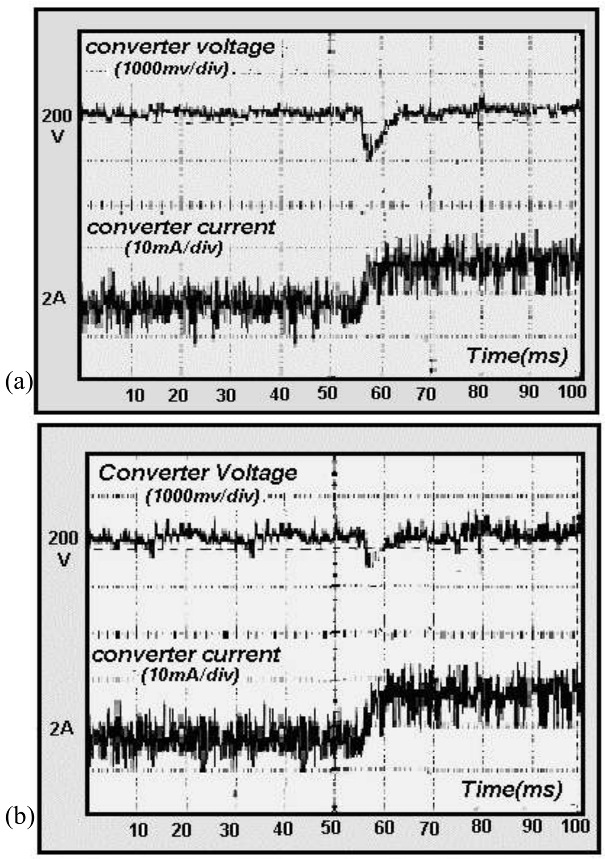

Fig. 11: The regulated output voltage and load current for a %0.5 step up change in load (a) for SSM controller (b) for ANN controller

ANN controller speed. A Matlab Simulink model is developed on base of small signal model of converter to train the neural network off-line. a three layer feed-forward

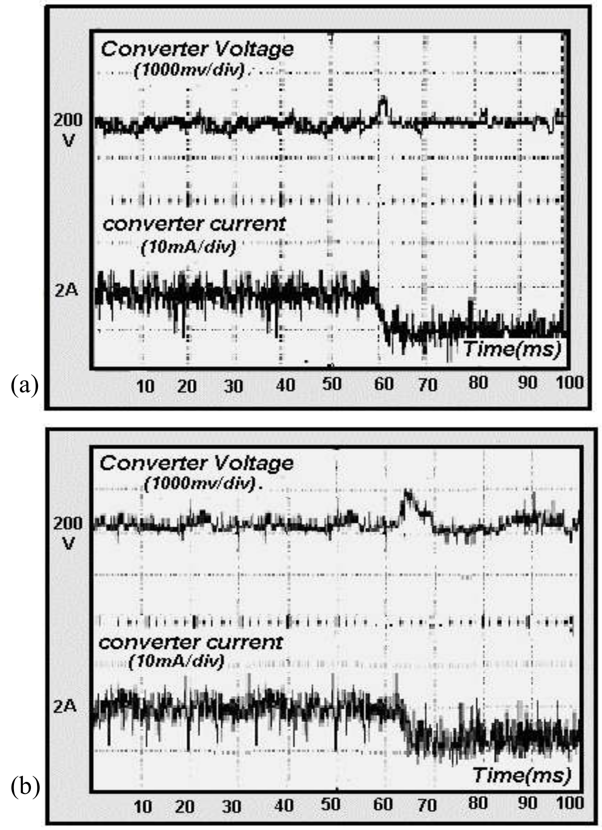

Fig. 12: The regulated output voltage and load current for a %0.5 step down change in load (a) for ANN controller (b) for SSM controller

neural network which has one hidden layer with 10 neurons was selected and the network weights are selected randomly with uniform distribution over the interval [-1, 1]. The total number of weights was 128 at first stage and this reduced to the 72 After activation of pruning process while still the ANN controller provide similar performances.

Experimental Results: In order to verify the results obtained theoretically, a 500W prototype was built as is shown in figure 10.

Experimental results showed that the difference between percentage of overshoot and settling time in output response in case of small changes in load current, for both SSM and ANN controllers is not noticeable. Although ANN controller provides slightly better system response performances in terms of Settling time, Overshoot and Rise time as depicted in figures 11 and 12. As illustrated in these figures, the converter output voltages, was regulated after about 5ms and 500mv (%0.25) over and undershoot for ANN controller in case

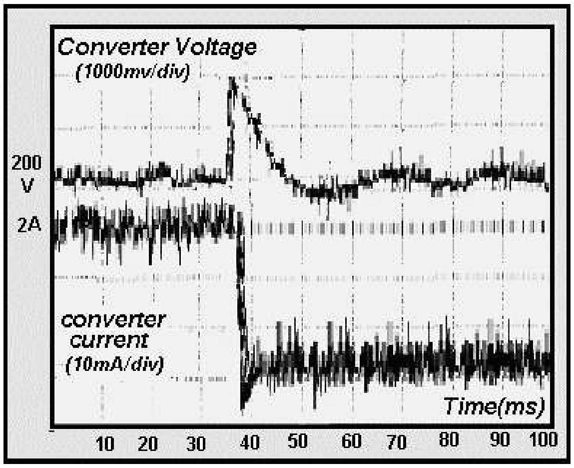

Fig. 13: The regulated output voltage and load current for a %1.5 step down change in load current for ANN controller

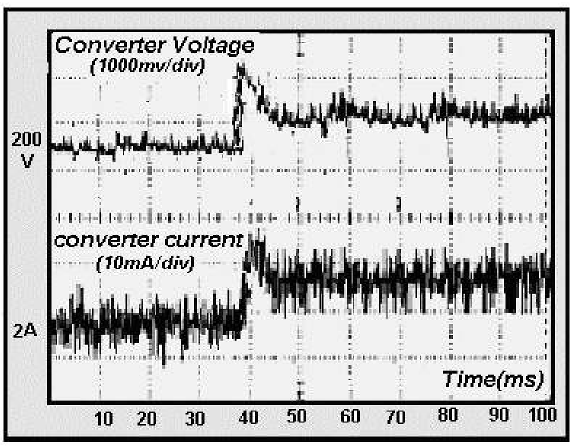

Fig. 14: The regulated output voltage and load current for a %0.5 step up change in reference voltage for ANN controller

of %0.5 step up or down changes in load current. While this time was about 10ms with a 1000mv (%0.5) overshoot for SSM controller for the same changes in load current. The difference was more considerable when changes in load current were increased. Figure 13 shows the regulation of output voltage for a change of %1.5 of rated current, in case of ANN controller. It is obvious that the percentage of overshoot increased in case of larger changes in load current. As can be seen in Figure 14, there was an overshoot in load current in case of step changes in reference voltage in both cases of ANN and SSM controllers. Experimental results for a range of step changes in load current showed that for larger changes, the percentage of overshoot and

(a)

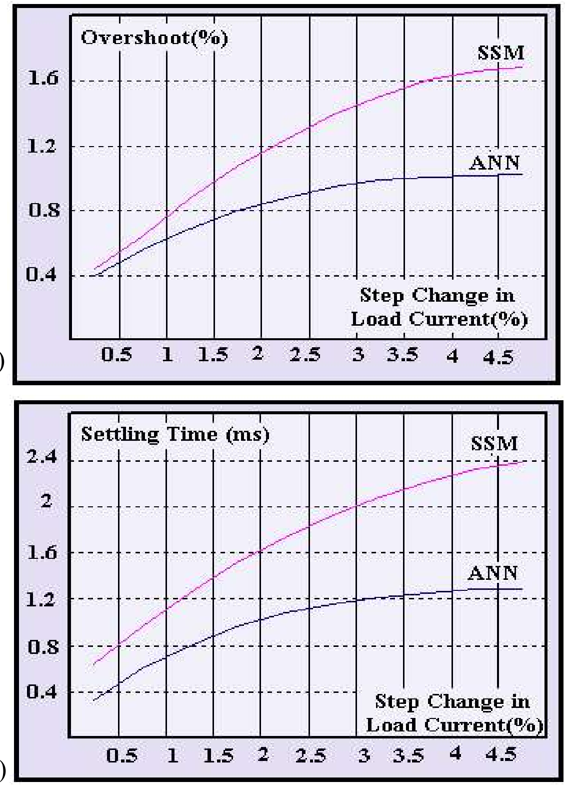

(b)

Fig. 15: Comparison between Overshoot (a) and Settling time (b) in output responses of ANN and SSM controllers

settling time increased for both controllers but this increase was more considerable for SSM controller. The results showed that the ANN controller provides better provides better response characteristics than SMM controller especially in case of large variations in load current. The graphs in figure 15 contrast the changes in overshoot and settling time for a range of step changes in load current for both controllers. It is obvious from the figures that the difference between responses for two controllers increased as the step changes go up. The difference also was more pronounced in case step changes in reference voltage.

CONCLUSION

It can be concluded that in general ANN controller provides better characteristic than the SSM controller in terms of overshoot, rise-time and settling time. This superiority was more noticeable for greater step changes in load current and reference voltage.

ACKNOWLEDGMENT

The authors would like to thank the R&D center of Islamic Azad University-Fasa Branch for the financial support of this research project.

REFERENCES

1. Ivensky, G., A. Kats and S. Ben-Yaakov, 1997. A Novel R C Model of Capacitive-Loaded Parallel and Series-Parallel Resonant DC-DC Converters. Proceedings of the 28th IEEE Power Electronics Specialists Conference, St. Louis, Missouri, USA, 2: 958-964.
2. Cavalcante, F.S. and J.W. Kolar, 2003. “Design of a 5kW High Output Voltage Series-Parallel Resonant DC-DC Converter,” in Proceedings of the 34th IEEE Power Electronics Specialists Conference, Acapulco, Mexico, 4: 1807-1814.
3. Garcia Soto, G., J. Gaysse and G.W. Baptiste, 2004. Variable Sampling Time Serial-Resonant Current Converter Control for a High-Voltage X-ray Tube Application. Proceedings of the 10th European Power Quality Conference, Nuremberg, Germany, pp: 972-977.
4. Sabate, J.A. and F.C.Y. Lee, 1991. Off-Line Application of the Fixed-Frequency Clamped-Mode Series Resonant Converter. IEEE Transactions on Power Electronics, 6(1): 39-47.
5. Aigner, H., 2005. Method for Regulating and/or Controlling a Welding Current Source with a Resonance Circuit, United States Patent 6849828.
6. Astrom, K.J. and B. Wittenmark, 1995. Adaptive Control. Second Edition, Addison-Wesley Publishing Company, Inc.,
7. Cecati, C., A. Dell'Aquila, M. Liserre, *et al.* A Passivity-Based Multilevel Active Rectifier with Adaptive Compensation for Traction *Applications*, IEEE Transactions on Industry Applications, 39: 5.
8. Ortega, R., A. Loría, P.J. Nicklasson and H. Sira-Ramirez, 1998. Passivity-based Control of Euler-Lagrange Systems: Mechanical, Electrical and Electromechanical Applications. Springer-Verlag, London, UK,
9. Xiao-Hua Yu, Weiming Li, Taufik" Design and implementation of a neural network controller for real-time adaptive voltage regulation